Analysis of Orthogonal Cutting Experiments Using Diamond-Coated Tools with Force and Temperature Measurements

Robert Ivester and Eric Whitenton
Engineering Laboratory
National Institute of Standards and Technology[1]
Gaithersburg, Maryland, USA

Jill Hershman and Kevin Chou
Mechanical Engineering Department
The University of Alabama
Tuscaloosa, Alabama, USA

Qiang Wu
Global Holemaking Systems Engineering
Kennametal Inc.
Latrobe, Pennsylvania, USA

ABSTRACT

Two dimensional (2D) orthogonal cutting experiments using diamond-coated tools were conducted with forces and tool-tip temperatures measured by dynamometry and infrared thermography, respectively. The objective of this study was to analyze cutting parameter effects on process behavior in diamond-coated tool machining. Special cutting tools and workpieces were prepared to realize orthogonal cutting. The specific cutting energy and the ratio of forces in the normal and cutting directions increased with decreasing uncut chip thickness. The tool temperatures generally increase with the uncut chip thickness. The specific cutting energy decreases slightly with the increase of the cutting speed. The tool temperatures increase significantly with the cutting speed, but level off at a higher cutting speed, 5 m/s. The effect of increasing the edge radius was to increase the specific cutting energy and the force ratio. The tool temperatures were lowest at the middle edge radius value and increase at both the smaller and larger edge radii.

INTRODUCTION

Synthetic polycrystalline diamond (PCD), made by high-pressure high-temperature sintering, is commonly used in the manufacturing industry to machine non-ferrous materials because of its exceptional mechanical and tribological properties. Increased uses of lightweight high-strength components and demands of dry machining have also promoted practices of diamond tools. However, processing and fabrications of PCD tools are of high cost. On the other hand, advanced surface engineering technologies such as chemical vapor deposition (CVD) have been widely explored for wear resistant applications including cutting tools [1,2]. There have been numerous advancements and studies of coating tools for machining, e.g., [3-5]. In addition, coating has an advantage in fabrications of tools with complex geometry. Diamond coatings, again owing to their extreme properties, have been investigated for cutting tool applications.

However, current practices for diamond coating cutting tools use off-the-shelf tools as substrates without any consideration of tool edge geometry or the effects of

---

[1] Commercial equipment is identified in order to adequately specify certain procedures. In no case does such identification imply recommendation or endorsement by the National Institute of Standards and Technology, nor does it imply that the materials or equipment are necessarily the best available for the purpose. Official contribution of the National Institute of Standards and Technology; not subject to copyright in the United States.

coating properties on machining. To effectively use diamond coated tools, it is necessary to understand the stress modifications around the tool edge due to the deposition process and during machining. Finite element simulations of machining processes have been advanced to study various aspects such as chip formation and cutting forces. On the other hand, there is a gap between the coating process/attributes and machining applications from the tool geometry perspective. Figure 1 below shows the relations between the tool edge geometry, coating properties, and machining response in diamond-coated tools. In particular, the cutting edge radius has conflicting effects on deposition stresses resulting from mismatched thermal expansions and on thermomechanical loading induced during machining.
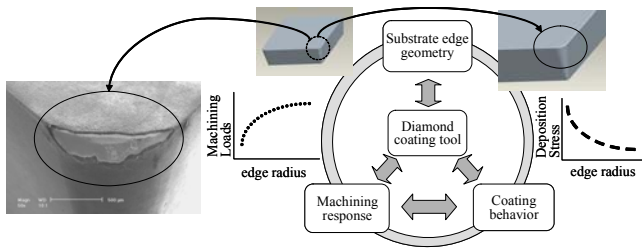

Figure 1. Conceptual illustration of the edge-geometry importance to diamond-coated tools for machining.

A previous study [6] has demonstrated that the cutting edge radius plays a crucial role on the performance of diamond-coated cutting tools, and further, the effect strongly depends upon machining conditions. It is found that by increasing the edge radius from 5 µm to 65 µm, the tool life of diamond-coated tools can be extended over 5 times in low-speed, high-feed machining conditions [6]. It is argued that the residual stress from diamond depositions at the coating-substrate interface, in particular, a normal tensile radial stress, results in poor adhesion. A sharp edge will inherit a high residual stress because of stress concentration, and thus, a more rounded edge may be favorable from coating adhesion consideration.

In an earlier numerical study [7], orthogonal cutting simulations with a diamond-coated tungsten carbide (WC) tool were developed to include residual stresses in the tool from depositions. The numerical study investigated the combined deposition and machining effects on the thermal and mechanical states of diamond-coated tools in 2D cutting. In particular, the role of the edge radius was emphasized because of its impact on the resultant interface stresses at different cutting conditions. First, finite element (FE) modeling was used to evaluate the deposition stresses in tools. Second, the tool with deposition stresses was imported into FE software to continue cutting simulations with different cutting conditions. The coating-substrate interface stresses were further analyzed. The stress/strain

and temperature fields of a diamond coated tool were analyzed, with the tool edge geometry, the coating thickness, and cutting parameters (cutting speed and uncut chip thickness) investigated. The interfacial stresses were extracted and compared to examine tool and process parameter effects.

In the work described in this paper, a special 2D cutting test-bed at NIST was utilized to conduct a set of machining experiments using specially prepared diamond-coated cutting tools. The test-bed is capable of measuring cutting force and tool temperature distribution. The objective of this work is to investigate the effect of cutting parameters in diamond-coated tool machining through analysis of experimentally measured process behavior and comparison to numerical studies.

EXPERIMENTAL DETAILS
Cutting Tool Preparations

The substrates used for diamond coating experiments were grooving type inserts (A4G-U-B-6) from Kennametal Inc. The insert material selected was fine-grain WC with 6 % cobalt by weight (K68 from Kennametal). Three levels of edge radii were selected for evaluations. The edge radius of cutting inserts prior to coating was measured by a commercial white-light interferometer with a 0.5X objective lens. Measurement results indicate that the uncoated average edge radii were: 5 µm, 25 µm, and 50 µm, with a k=2 expanded measurement uncertainty of 1 µm. To facilitate temperature distribution measurements, the side relief surface near the cutting edge was precision-ground flat and perpendicular to the cutting edge.

For the coating process, diamond films were deposited using a high-power microwave plasma-assisted CVD process. A gas mixture of methane in hydrogen was used as the feedstock gas. Nitrogen, maintained at a certain ratio to methane, was inserted into the gas mixture to obtain nanostructures by preventing cellular growth. The nominal pressure was 12 kPa and the nominal substrate temperature was 800 °C. The coated inserts were further inspected by the interferometer to measure the edge radius and to estimate the coating thickness. The coating thicknesses of 20 µm and 25 µm increased the final edge radii accordingly. The average surface roughness, R_a, of the tools after cutting was approximately 0.5 µm.

Workpieces

The workpieces were thin disks (127 mm diameter, 3 mm thick) precision machined from a bar stock made of A356 aluminum alloy that was cast and heat treated. The FE cutting simulations used material properties for this particular alloy as reported in the literature [8].

The 2D cutting test-bed was modified from a computer numerical control (CNC) super-abrasive machining center with the addition of multiple sensors. Figure 2a shows the machine and Figure 2b shows the cutting tool and workpiece arrangement in the machine. Figure 3 depicts (a) the setup of a diamond-coated tool and the disk-shaped workpiece and (b) the side view of a diamond-coated tool tip. A digital oscilloscope records the dynamometer signals at a sampling rate of 2 MHz before down-sampling to 500 Hz for analysis. A high-speed visible light camera (shutter speed of 30,000 frames per second (fps), integration time of 33 μs) and a medium-speed infrared camera (600 fps shutter speed, 10 μs to 25 μs integration time, 3 μm to 5 μm wavelength) simultaneously record the cutting process. The disk-shaped workpiece rotates on the horizontal spindle and moves on a vertical axis (feed direction). Synchronizing the dynamometer, visible light camera, and infrared camera signals by reading each signal with an oscilloscope at 2 MHz sampling rate provides confidence the signals represent nearly identical instances in time. The detail of machine and instruments can be found in [9].
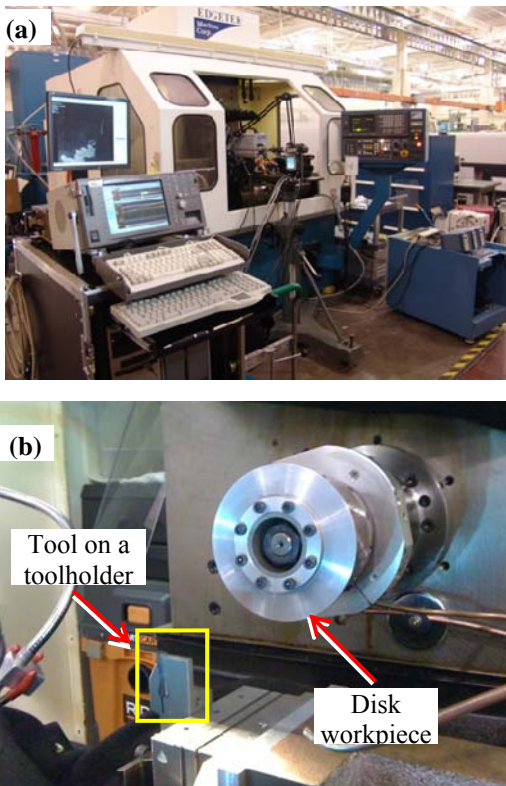

Figure 2. (a) 2D orthogonal cutting test-bed, and (b) Workpiece and tool arrangement in the machine.
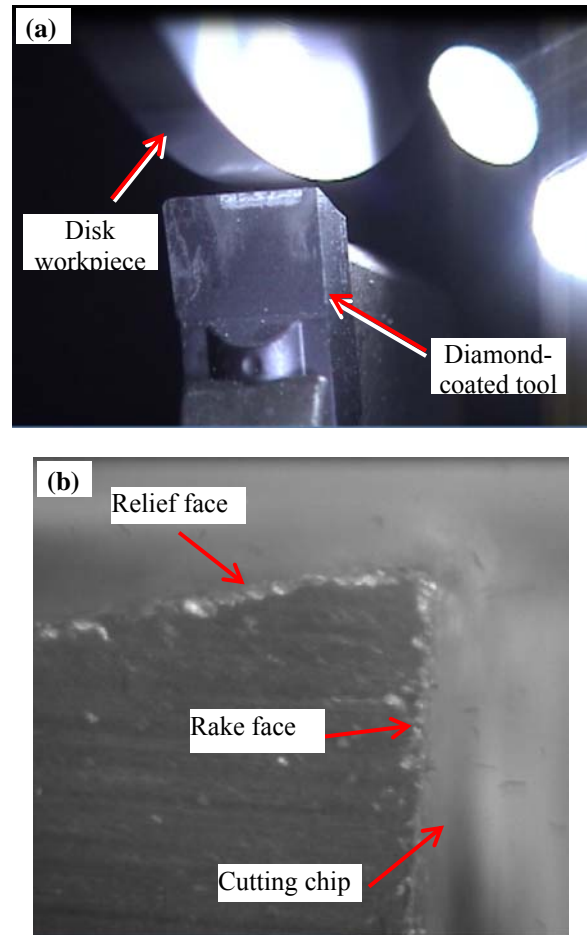

Figure 3. (a) Close-up view of tool and workpiece setup, and (b) Side view of a diamond-coated tool tip.

Testing Parameters

The toolholder used was A4SML 160624, 25.4 mm steel shank holder. The resulting nominal cutting geometry was 7° of rake angle and 4° of relief angle. The uncut chip thickness (h) values were 0.05 mm, 0.15 mm and 0.30 mm. The cutting speed (V) tested included 2 m/s, 5 m/s, and 10 m/s. The linear cutting length was over 5 revolutions to ensure realization of the full uncut chip thickness. Machining was conducted at room temperature without coolant. In each cutting test, cutting forces and tool temperatures were acquired and further analyzed using MATLAB scripts developed at NIST [10]. For infrared temperature measurements, the emissivity of diamond-coated tools was determined by heating up the tools to a range of temperatures while simultaneously measured by a thermocouple and the infrared camera. The emissivity was between 0.72 and 0.79 (k=2 expanded measurement uncertainty of 0.02) for the temperature range of 150 °C to 200 °C. Linear extrapolation was used for the temperature range outside of the emissivity testing range.

RESULTS AND DISCUSSION

The post-processed data from the experiments were plotted and compared. The section below presents the cutting variable plots/contours for different cutting conditions. Figure 4 shows the cutting force history from a typical cutting test (5 m/s cutting speed and 0.15 mm uncut chip thickness) with steady state forces of approximately 400 N and 200 N for the cutting and thrust components, respectively. The small side force indicates that the orientation of the cutting edge deviates only slightly from the axis of rotation of the disk. Figure 5 shows the temperature, at a specific location on the tool versus the cutting time. The inset thermal images in Figure 5 show the tool temperature distributions corresponding to the indicated times. The temperature contours during the steady state cutting period were averaged to obtain the mean temperature distribution at the tool tip area (inset under the curve in Figure 5).
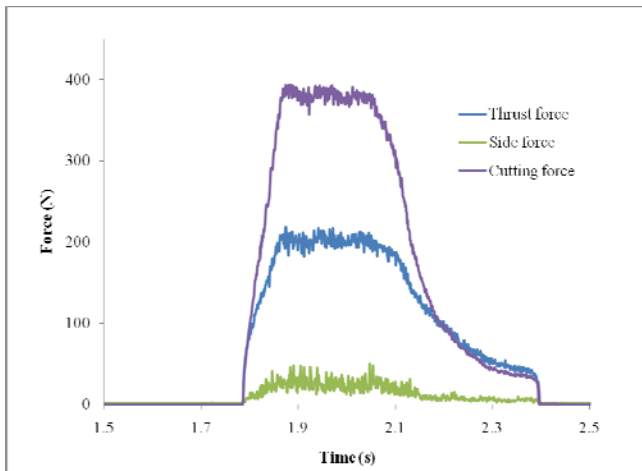

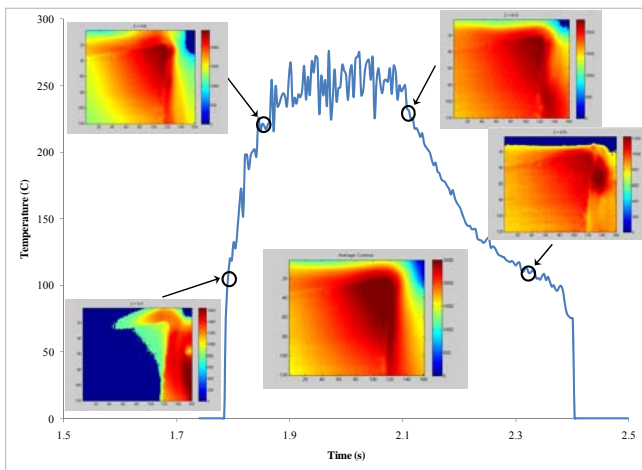**Figure 4.** Cutting force history from one test.

Figure 5. Temperature history at a location close to the tool tip; inserts are thermal images at different times.

(1) Uncut Chip Thicknesses Effect

Figure 6a shows how the specific cutting energy (E) varied with the uncut chip thickness at different edge radii with a cutting speed of 5.0 m/s. E is in the range of 700 MPa to 1200 MPa. The trend agrees with conventional knowledge, E increasing with decreasing uncut chip thickness (h), and the effect is manifested at a larger edge radius (50 µm substrate), in particular, at very low uncut chip thickness (0.05 mm). Figure 6b shows the ratio of the cutting force to the thrust force (force ratio) varied with the uncut chip thickness at different edge radii. The force ratio also significantly increases with decreasing h. It is observed that a ratio as high as 0.9 may occur at a large edge radius and small h. The condition of h = 0.15 mm was duplicated (2 data points for 25 µm and 50 µm edge radii in the figures) and the results show reasonable repeatability.
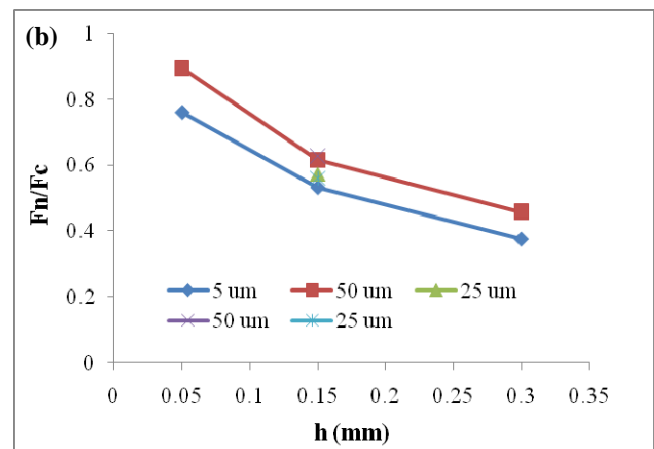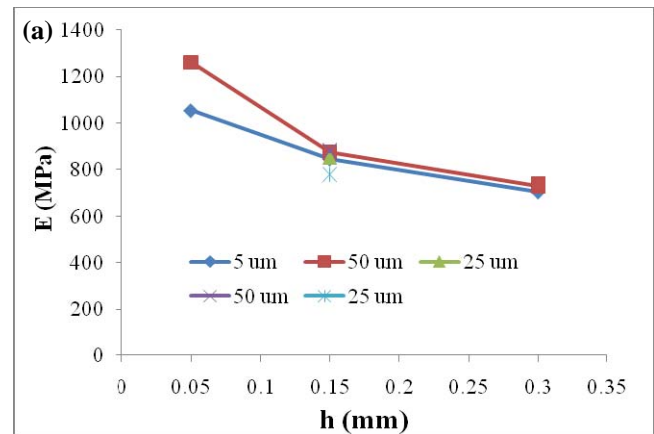

Figure 6. (a) Specific cutting energy, and (b) Cutting force ratio vs. uncut chip thickness, h, for different edge radii (v=5 m/s).

Figure 7 displays the temperature distributions at the tool tip (approximately 1 mm wide field of view) at different uncut chip thicknesses for the case of 5 µm edge

radius. The tool edge profiles are recognizable from the contours. It is observed that tool temperatures generally increase with the uncut thickness. The maximum temperature of around 300 °C occurred at 0.3 mm h vs. less than 200 °C for 0.05 mm h. Note that the entire temperature fields were converted to true temperatures using the linear temperature-emissivity relationship of the tools (diamond-coated tools). Therefore, the portions of the temperature fields outside of the tool profile are not correctly represented.
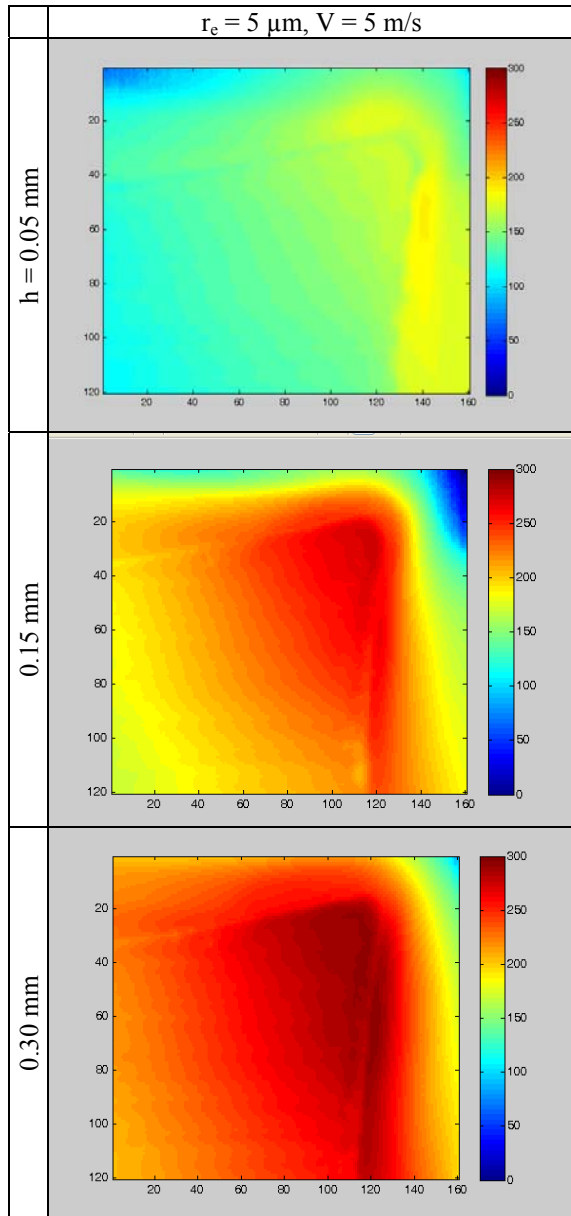
Figure 7. Cutting tool temperature contours (°C) at different uncut chip thicknesses, h (x and y scales in pixels).

(2) Cutting Speed Effect

Figure 8a shows the changes in specific cutting energy with cutting speed at different edge radii for an uncut thickness of 0.15 mm. E is in the range of 800 MPa to 1000 MPa. It is also observed that E decreases slightly with the increase of the cutting speed (V). The effect of the edge radius is small for the range of conditions tested. Similarly, Figure 8b shows changes in the force ratio with cutting speed at different edge radii. The cutting force ratio also decreases slightly with increasing cutting speed, ranging between 0.55 A and 0.7. A larger edge radius effect can be noted as well.
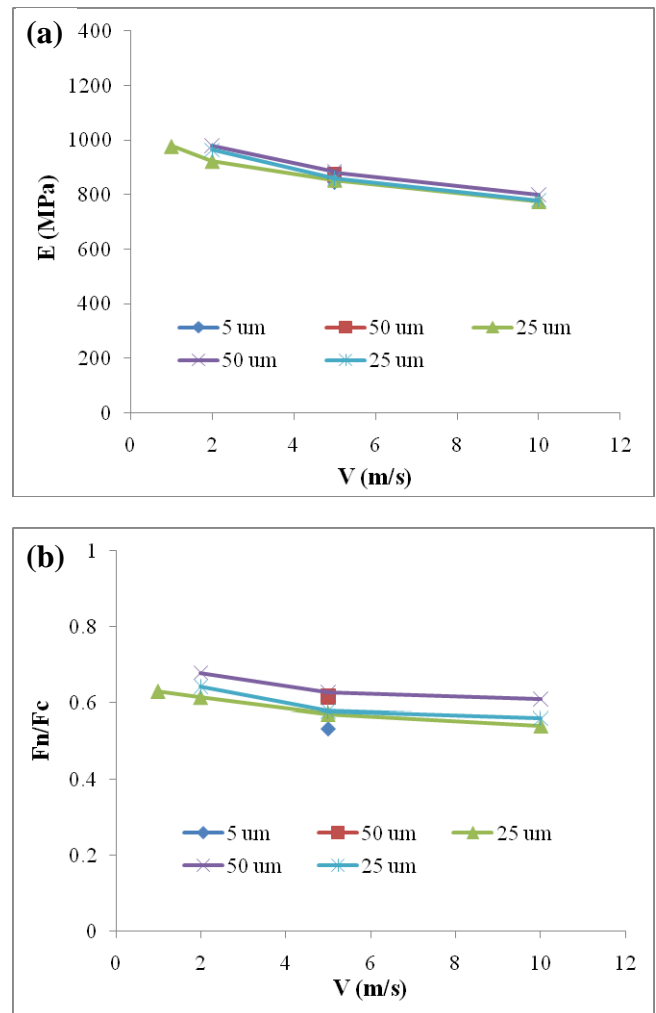

Figure 8. (a) Specific cutting energy, and (b) Cutting force ratio vs. cutting speed for different edge radii (h=0.15 mm).

Figure 9 displays the effect of the cutting speed on tool tip temperatures at an edge radius of 25 μm. It is observed that tool temperatures increase with cutting speed up to 5 m/s and level off from 5 m/s to 10 m/s. The maximum tool temperatures are in the range of about 175 °C for 1 m/s to about 275 °C for 5 m/s and 10 m/s.
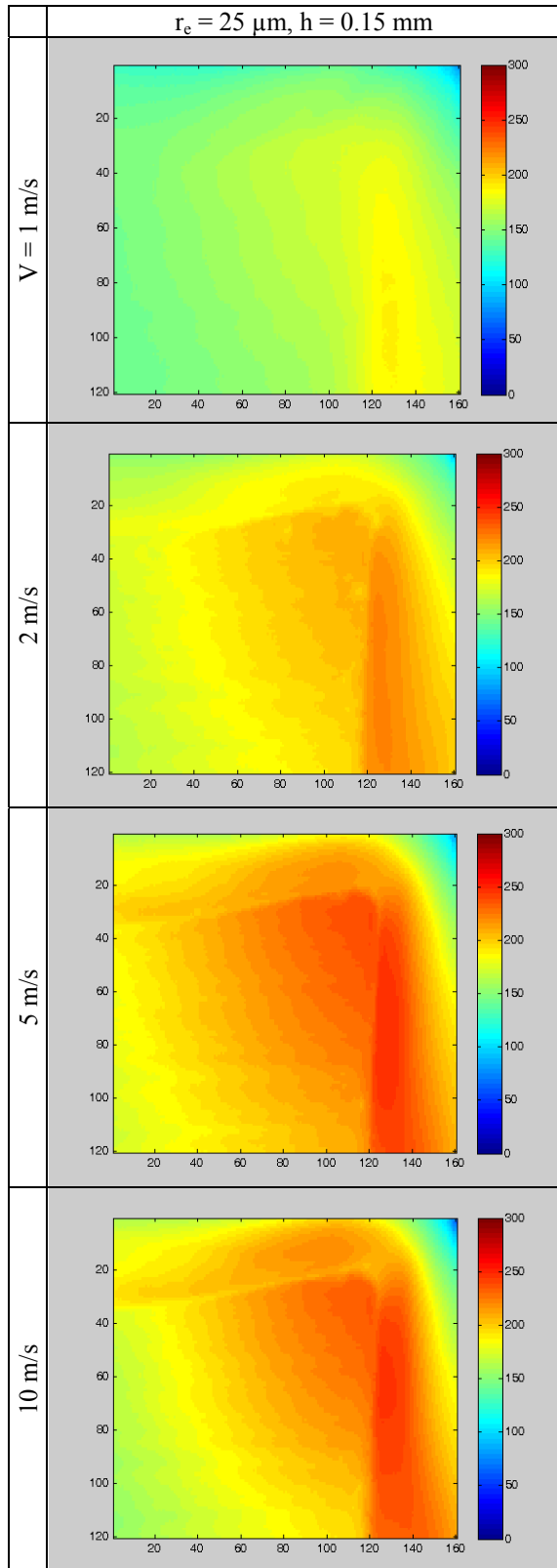
Figure 9. Cutting tool temperature contours (°C) at different cutting speeds (x and y scales in pixels).

(3) Edge Radius Effect on Cutting Tool Temperatures

The measured effects of the edge radius on the specific cutting energy and the force ratio are significant, especially at a smaller uncut thickness. The measured tool temperatures (Figure 10 below) appear to be minimized at 25 µm, and larger at both 5 µm and 50 µm.
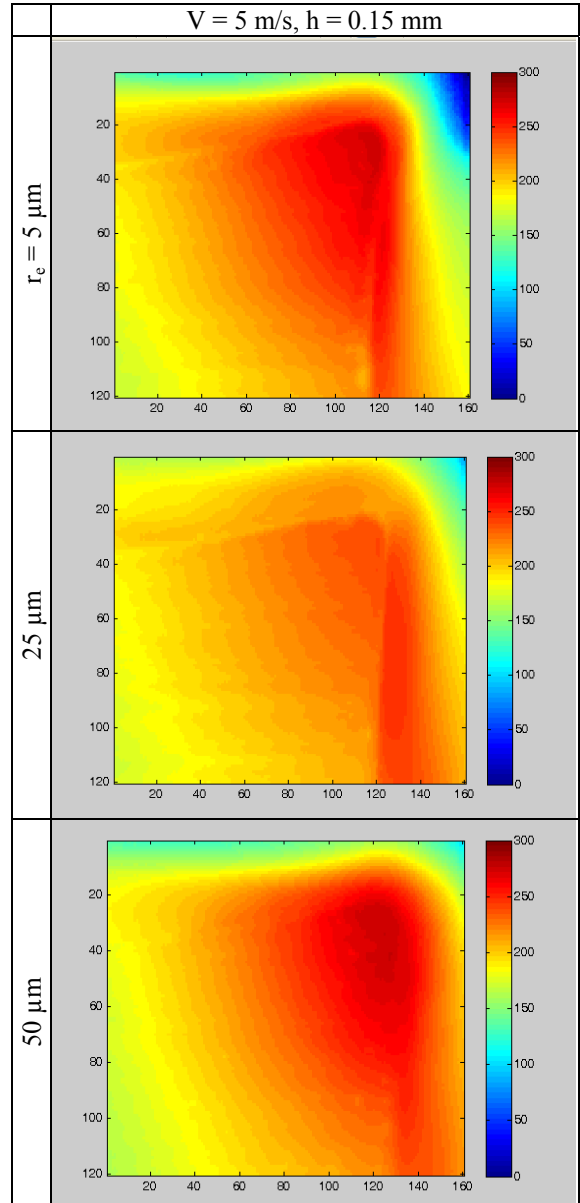

Figure 10. Cutting tool temperature contours (°C) at different edge radii (x and y scales in pixels).

Simulation Result Example

FE simulations of 2D cutting with a diamond-coated tool were realized using ABAQUS software. The simulations include a deposition stress analysis with a given deposition temperature and coating and substrate properties, and a subsequent cutting simulation using the arbitrary Lagrangian Eulerian scheme including the tool with the inherited deposition stresses and a workpiece with given material constitutive model and frictional coefficient. The simulation was conducted in the explicit dynamic analysis mode to reach a steady state chip formation. The details of the simulation procedure can be found in a previous publication [7]. The results from an example (25 μm edge radius, 20 μm coating thickness, 5 m/s cutting speed, and 0.15 mm uncut chip thickness) are shown here. Figure 11 plots the von Mises stress contours during cutting, (a) in the workpiece and chip and (b) in the diamond-coated tool. It is noted that the stress level in the primary shear zone is on the order of 300 MPa to 400 MPa; however, the tool has a very high localized stress, over 7 GPa, in the edge-flank transition area. Note that the residual stress from the diamond deposition can be as high as 4 GPa, as was observed from the previous analysis. Cutting forces calculated from the simulation are 162 N and 72 N, respectively, for 1 mm width of cut, which are comparable to the experimental results (128 N and 73 N per mm width of cut). Figure 12 plots the temperature contour, (a) tool-chip-workpiece, and (b) only tool. The maximum tool temperature is around 330 °C vs. 275 °C from the experiment.
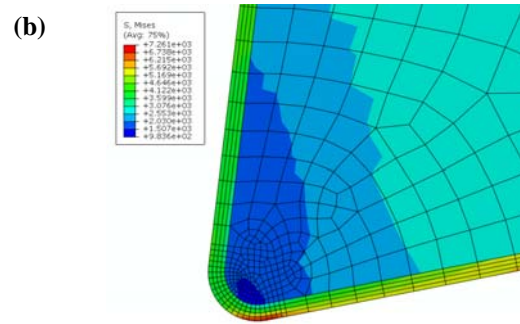
(b)

Figure 11. Stress contour from cutting simulations: (a) Workpiece and chip, and (b) Tool alone (unit: MPa).

(a)

(b)

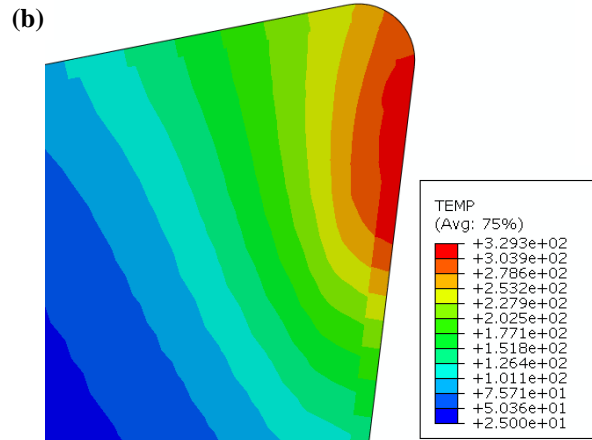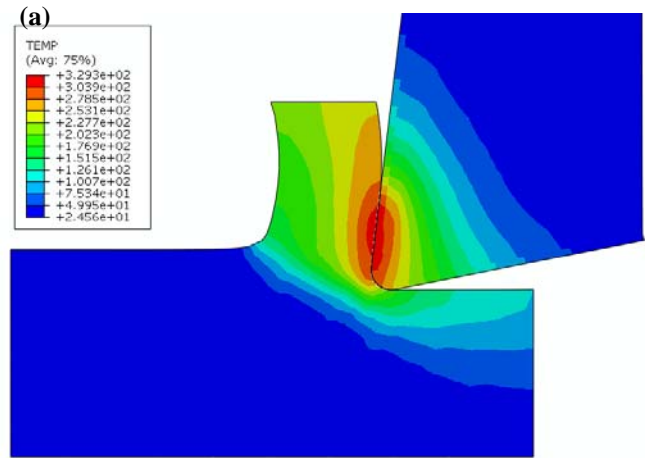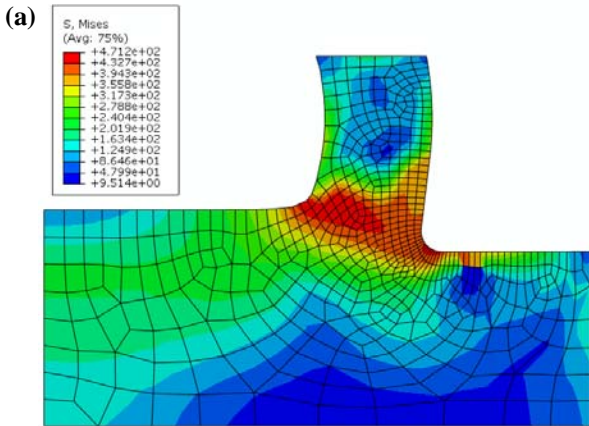**Figure 12.** Cutting tool tip temperature contours: (a) Overall, and (b) Tool alone (Unit: °C).

CONCLUSIONS

Analysis of orthogonal cutting with force and temperature measurements was conducted using the experimental setup at NIST, and a comparison of these measurements to numerical studies was performed. The experimental data were processed to evaluate the effects of process parameters and the tool edge radius. The initial testing sets reveal the major findings summarized below.

(a)

(1) As the uncut chip thickness increases, the tool temperature increases and the specific cutting energy and normal vs. cutting force ratio decrease.
(2) As the cutting speed increases, the specific cutting energy decreases slightly, and the tool temperatures increase substantially.
(3) The effect of the edge radius on the specific cutting energy and the force ratio is noticeable; however, the effect on the tool temperatures is inconsistent with classical theory.
(4) The preliminary comparison between the experimental results and simulations indicates reasonable agreement.

The first two findings are consistent with classical metal cutting literature [11]. The third finding indicates a need for further investigation to better understand the underlying phenomena.

For future work, more extensive testing, including systematic repeatability evaluations, a larger uncut chip thickness, and uncoated tool cutting comparisons will be performed. In addition, more thorough quantitative comparisons with FE cutting simulation results will be analyzed.

ACKNOWLEDGEMENTS

REFERENCES

[1] Kustas, F.M., Fehrehnbacher, L.L., and Komanduri, R., 1997, "Nanocoatings on Cutting Tools for Dry Machining," *Annals of CIRP*, **46**(1), pp. 39-42.

[2] Arumugam, P.U., Malshe, A.P., and Batzer, S.A., 2006, "Dry Machining of Aluminum–silicon Alloy Using Polished CVD Diamond-coated Cutting Tools Inserts," *Surface and Coatings Technology*, **200**(11), pp. 3399-3403.

[3] Grzesik, W., Zalisz, Z., and Nieslony, P., 2002, **"**Friction and Wear Testing of Multilayer Coatings on Carbide Substrates for Dry Machining Applications**,**" *Surface and Coatings Technology*, **155**(1), pp. 37-45.

[4] Balaji, A.K. and Jawahir, I.S., 2001, "A Machining Performance Study in Dry Contour Turning of Aluminum Alloys with Flat-faced and Grooved Diamond Tools," *Machining Science and Technology*, **5**(2), pp. 269-289.

[5] Bouzakis, K.-D., Hadjiyiannis, S., Skordaris, G., Mirisidis, I., Michailidis, N., Efstathiou, K., Pavlidou, E., Erkens, G., Cremer, R., Rambadt, S., and I. Wirth, 2004, "The Effect of Coating Thickness, Mechanical Strength and Hardness Properties on the Milling Performance of PVD Coated Cemented Carbides Inserts," *Surface and Coatings Technology,* **177-178***,* pp. 657-664.

[6] Qin, F., K. Chou, D. Nolen, R.G. Thompson, and W. Ni, "Cutting Edge Radius Effects on Diamond Coated Tools," Transactions of NAMRI/SME, **37**, pp. 653-660, 2009.

[7] Qin, F. and K. Chou, "2D Cutting Simulations with a Diamond-coated Tool Including Deposition Residual Stresses," Transactions of NAMRI/SME, **38**, pp. 1-8, 2010.

[8] Sartkulvanich, P. H. Sahlan, and T. Altan, 2007, "A Finite Element Analysis of Burr Formation in Face Milling of a Cast Aluminum Alloy," *Machining Science and Technology*, **11**, pp. 157-181.

[9] Heigel, J.C, R.W. Ivester and E.P. Whitenton, "Temperature Measurements of Segmented Chips Using Dual-Spectrum High-Speed Microvideography," Transactions of NAMRI/SME, **36**, pp. 73-80, 2008.

[10] Ivester, R.W. "Tool Temperatures in Orthogonal Cutting of Alloyed Titanium," Proceedings of NAMRI/SME, **39**, 2011.

[11] Shaw, M. C., Metal Cutting Principles, Oxford University Press, New York, NY, 1984.